

Characteristics of American Put Options

Ritchie Ling, Linlong (Liam) Wu , Alice Yin

October 2022

Abstract

This paper derives a numerical method to evaluate an American put option using the Cos-Ross Rubinstein binomial pricing model, exploring its exercise boundary and the hedging strategy. Simulations were performed to explore the characteristics of the American put option, such as the kernel density estimate of the profit and losses and the distribution of the exercise time. The impact of the parameter change on the above results was also examined and discussed.

1 Introduction

The Fundamental Theorem of Asset Pricing (FTAP) states that a market is arbitrage-free if and only if there exists a risk-neutral probability measure that is equivalent to the original probability measure. Risk neutral measure is a probability measure such that the price of an asset is exactly equal to the discounted expectation of future prices under the risk-neutral probability measure. The risk-neutral measure does not depend on the actual return of the asset.

The Cox-Ross-Rubinstein binomial pricing model is a risk-neutral valuation which provides a numerical method to evaluate financial derivative prices in a discrete-time setting. Under the CRR model setting, a fixed time horizon T is divided into N small subperiods. The asset price movement for each subperiod follows a Bernoulli distribution with a risk-neutral probability q , representing the probability of an up-movement. In each step, the asset price S_t either goes up to uS_t with a probability of q , or goes down to dS_t with a probability of $(1 - q)$, where u and d are a function of volatility and subperiod length. Once the asset price tree is constructed, one can work backwards to derive the price for the derivative that is written on this asset. The valuation result would converge to the Black-Scholes pricing model result as the number of subperiods approached infinity.

The following are the settings for this project:

An asset price process $S_t = (S_{t_k})_{k \in 0,1,\dots,N}$ (with $t_k = k\Delta t$ and $\Delta t = \frac{T}{N}$, for a fixed N) are given by the stochastic dynamics

$$S_{t_k} = S_{t_{k-1}} e^{r\Delta t + \sigma\sqrt{\Delta t}\epsilon_k}$$

where $\epsilon_k \in (+1, -1)$ and

$$\mathbb{P}(\epsilon_k \pm 1) = \frac{1}{2} \left(1 \pm \frac{(\mu - r) - \frac{1}{2}\sigma^2}{\sigma} \sqrt{\Delta t} \right)$$

Assuming $r \leq 0$ and $\sigma > 0$ are constants.

Next, let $B = (B_{t_k})_{k \in 0,1,\dots,N}$ denote the bank account with $B_t = e^{rt}$. According to FTAP, one can construct a risk-neutral measure by using B as a numeraire.

This project explores the characteristics of an at-the-money American put option under the given assumptions. A at-the-money option refers to the situation that the strike price is identical to the current market price of the underlying asset. An American put option allows the holder to have the right to exercise

the option at any time point up to and including the expiration date, whereas the holder can only exercise the European put at maturity.

First, we derived the distribution of the log return of the asset and the limiting distribution of the asset pricing under different risk-neutral measures. The derived results are used to construct a CRR binomial pricing tree for the stock price and determine the option's price and exercise boundary. We've derived a hedging strategy as a function of the spot price S for selected time points and compared it with the hedging strategy of a European put. Then, we performed simulations to obtain a kernel density estimate of the profit and loss and the distribution of the exercise time. We also investigated the impact of different realized volatility on the distribution of profit and loss and exercise time of the option.

2 Methodology

2.1 Assumptions

(1) Stock distribution

In this section we are going to find the distribution of stock price in a CRR tree. We use the property of moment generating function to approach the asset which could be expressed as a log normal distribution. Given the relation between two terms: S_{t_k} and $S_{t_{k-1}}$, we can easily derive the general form equation of S_{t_k} .

$$\begin{aligned} S_{t_k} &= S_{t_{k-1}} e^{r\Delta t + \sigma\sqrt{\Delta t}\epsilon_k} \\ S_{t_k} &= e^{\sum_{k=1}^N r\Delta t + \sigma\sqrt{\Delta t}\epsilon_k} \end{aligned}$$

Then, we have $X^{(N)} = \log\left(\frac{S_T}{S_0}\right) = \sum_{k=1}^N r\Delta t + \sigma\sqrt{\Delta t}\epsilon_k = rT + \sum_{k=1}^N \sigma\sqrt{\Delta t}\epsilon_k$, since $N\Delta t = T$. We calculated the MGF for $X^{(N)}$ as follows:

$$\begin{aligned} \mathbb{E}^P[e^{uX^{(N)}}] &= \mathbb{E}^Q[e^{u(rT + \sum_{k=1}^N \sigma\sqrt{\Delta t}\epsilon_k)}] \\ &= \mathbb{E}^P[e^{urT + u\sum_{k=1}^N \sigma\sqrt{\Delta t}\epsilon_k}] \\ &= e^{urT} \mathbb{E}^P[e^{u\sum_{k=1}^N \sigma\sqrt{\Delta t}\epsilon_k}] \\ &= e^{urT} \prod_{k=1}^N \mathbb{E}^P[e^{u\sigma\sqrt{\Delta t}\epsilon_k}] \quad (\text{Since } \epsilon_k \text{ are iid}) \\ &= e^{urT} (\mathbb{E}^P[e^{u\sigma\sqrt{\Delta t}\epsilon_1}])^N \end{aligned}$$

Since $\epsilon_k \in \{-1, +1\}$ and also $P(\epsilon_k = \pm 1) = \frac{1}{2}(1 \pm \frac{(\mu-r)-\frac{1}{2}\sigma^2}{\sigma}\sqrt{\Delta t})$, with $r \geq 0$ and also $\sigma > 0$

Using Taylor expansion on the exponential function, we will have the following with the approximation for the MGF of $X^{(N)}$

$$\begin{aligned} e^{u\sigma\sqrt{\Delta t}} &= 1 + u\sigma\sqrt{\Delta t} + \frac{1}{2}u^2\sigma^2\Delta t + O(\Delta t) \\ e^{-u\sigma\sqrt{\Delta t}} &= 1 - u\sigma\sqrt{\Delta t} + \frac{1}{2}u^2\sigma^2\Delta t + O(\Delta t) \end{aligned}$$

$$\begin{aligned}
\mathbb{E}^P[e^{\sigma\sqrt{\Delta t}\epsilon_k}] &= e^{u\sigma\sqrt{\Delta t}}P(\epsilon_k = 1) + e^{-u\sigma\sqrt{\Delta t}}P(\epsilon_k = -1) \\
&= e^{u\sigma\sqrt{\Delta t}}\frac{1}{2}\left(1 + \frac{(\mu - r) - \frac{1}{2}\sigma^2}{\sigma}\sqrt{\Delta t}\right) + e^{-u\sigma\sqrt{\Delta t}}\frac{1}{2}\left(1 - \frac{(\mu - r) - \frac{1}{2}\sigma^2}{\sigma}\sqrt{\Delta t}\right) \\
&= [1 + u\sigma\sqrt{\Delta t} + \frac{1}{2}u^2\sigma^2\Delta t + O(\Delta t)]\frac{1}{2}\left(1 + \frac{(\mu - r) - \frac{1}{2}\sigma^2}{\sigma}\sqrt{\Delta t}\right) \\
&\quad + [1 - u\sigma\sqrt{\Delta t} + \frac{1}{2}u^2\sigma^2\Delta t + O(\Delta t)]\frac{1}{2}\left(1 - \frac{(\mu - r) - \frac{1}{2}\sigma^2}{\sigma}\sqrt{\Delta t}\right) \\
&= \frac{1}{2}\left[1 + \frac{(\mu - r) - \frac{1}{2}\sigma^2}{\sigma}\sqrt{\Delta t} + u\sigma\sqrt{\Delta t} + u(\mu - r - \frac{1}{2}\sigma^2)\Delta t + \frac{1}{2}u^2\sigma^2\Delta t + \frac{1}{2}u^2\sigma(u - r - \frac{1}{2}\sigma^2)\Delta t^{\frac{3}{2}}\right. \\
&\quad \left.+ 1 - \frac{(\mu - r) + \frac{1}{2}\sigma^2}{\sigma}\sqrt{\Delta t} - u\sigma\sqrt{\Delta t} + u(\mu - r - \frac{1}{2}\sigma^2)\Delta t + \frac{1}{2}u^2\sigma^2\Delta t \right. \\
&\quad \left. - \frac{1}{2}u^2\sigma(u - r - \frac{1}{2}\sigma^2)\Delta t^{\frac{3}{2}}\right] + O(\Delta t) \\
&= 1 + u((\mu - r - \frac{1}{2}\sigma^2) + \frac{1}{2}u^2\sigma^2)\Delta t + O(\Delta t) \\
&= e^{u((\mu - r - \frac{1}{2}\sigma^2) + \frac{1}{2}u^2\sigma^2)\Delta t}
\end{aligned}$$

Therefore,

$$\begin{aligned}
\mathbb{E}^P[e^{uX^{(N)}}] &= e^{urT}[e^{u((\mu - r - \frac{1}{2}\sigma^2) + \frac{1}{2}u^2\sigma^2)\Delta t}]^N \\
&= e^{urT}e^{u((\mu - r - \frac{1}{2}\sigma^2) + \frac{1}{2}u^2\sigma^2)T} \\
&= e^{u(\mu - \frac{1}{2}\sigma^2)T + \frac{1}{2}u^2\sigma^2T}
\end{aligned}$$

Since the MGF of normal distribution $Z \sim N(a, b)$ is $\mathbb{E}[e^{uZ}] = e^{au + \frac{1}{2}\sigma u^2}$

$$\begin{aligned}
X^{(N)} &= \log\left(\frac{S_T}{S_0}\right) \stackrel{\mathbb{P}}{\sim} \mathcal{N}\left((\mu - \frac{1}{2}\sigma^2)T, \sigma\sqrt{T}\right) \\
X^{(N)} &\xrightarrow[N \rightarrow \infty]{d} (\mu - \frac{1}{2}\sigma^2)T + \sigma\sqrt{T}Z, \text{ and } Z \stackrel{\mathbb{P}}{\sim} \mathcal{N}(0, 1) \\
S_T &= S_0 e^{X^{(N)}}
\end{aligned}$$

(2) Risk-neutral probability

Risk-neutral probabilities are probabilities of possible future outcomes that have been adjusted for risk. This can also help us to figure out fair prices for assets.

To find the limiting distribution of $X^{(N)}$ under the martingale measure induced by using the asset B as a numeraire. According to the FTAP:

$$\mathbb{E}^{\mathbb{Q}}\left[\frac{S_{tk}}{B_{tk}} \middle| \mathcal{F}_{k-1}\right] = \frac{S_{tk-1}}{B_{tk-1}}$$

Set $q_b = \mathbb{Q}(k=1)$, and $q_s = \mathbb{Q}^S(k=1)$

$$\begin{aligned}
\frac{S_{t,k}}{B_{t,k}} &= q_b \frac{S_{t+1,k}}{B_{t+1,k}} + (1 - q_b) \frac{S_{t+1,k+1}}{B_{t+1,k+1}} \\
&= \frac{S_{t,k} e^{r\Delta t + \sigma\sqrt{\Delta t}}}{B_{t,k} e^{r\Delta t}} q_b + \frac{S_{t,k} e^{r\Delta t - \sigma\sqrt{\Delta t}}}{B_{t,k} e^{r\Delta t}} (1 - q_b) \\
q_b &= \frac{1 - e^{-\sigma\sqrt{\Delta t}}}{e^{\sigma\sqrt{\Delta t}} - e^{-\sigma\sqrt{\Delta t}}} \\
&= \frac{1 - (1 - \sigma\sqrt{\Delta t} + \frac{1}{2}\sigma^2\Delta t + O(\Delta t))}{(1 + \sigma\sqrt{\Delta t} + \frac{1}{2}\sigma^2\Delta t + O(\Delta t)) - (1 - \sigma\sqrt{\Delta t} + \frac{1}{2}\sigma^2\Delta t + O(\Delta t))} \\
&= \frac{1}{2} - \frac{1}{4}\sigma\sqrt{\Delta t} + O(\Delta t)
\end{aligned}$$

Then we use the same method in assumption (1) to calculate the MGF over \mathbb{Q} of X_N

$$\begin{aligned}
\mathbb{E}^{\mathbb{Q}}[e^{u\epsilon_k}] &= e^{u\sigma\sqrt{\Delta t}}(\frac{1}{2} - \frac{1}{4}\sigma\sqrt{\Delta t}) + e^{-u\sigma\sqrt{\Delta t}}(\frac{1}{2} + \frac{1}{4}\sigma\sqrt{\Delta t}) + O(\Delta t) \\
&= (1 + u\sigma\Delta t + \frac{1}{2}u^2\sigma^2\Delta t)(\frac{1}{2} - \frac{1}{4}\sigma\sqrt{\Delta t}) + (1 - u\sigma\Delta t + \frac{1}{2}u^2\sigma^2\Delta t)(\frac{1}{2} + \frac{1}{4}\sigma\sqrt{\Delta t}) + O(\Delta t) \\
&= 1 + (-\frac{1}{2}u\sigma^2 + \frac{1}{2}u^2\sigma^2)\Delta t + O(\Delta t) \\
&= e^{(-\frac{1}{2}u\sigma^2 + \frac{1}{2}u^2\sigma^2)\Delta t}
\end{aligned}$$

Then,

$$\begin{aligned}
\mathbb{E}^{\mathbb{Q}}[e^{uX^{(N)}}] &= e^{urT} (e^{(-\frac{1}{2}u\sigma^2 + \frac{1}{2}u^2\sigma^2)\Delta t})^N \\
&= e^{urT} e^{(-\frac{1}{2}u\sigma^2 + \frac{1}{2}u^2\sigma^2)T} \\
&= e^{u(r - \frac{1}{2}\sigma^2)T + \frac{1}{2}u^2\sigma^2T} \\
X^{(N)} &\overset{\mathbb{Q}}{\approx} \mathcal{N}((r - \frac{1}{2}\sigma^2)T, \sigma\sqrt{T}) \\
X^{(N)} &\xrightarrow[N \rightarrow \infty]{d} (r - \frac{1}{2}\sigma^2)T + \sigma\sqrt{T}Z, \quad Z \overset{\mathbb{Q}}{\approx} \mathcal{N}(0, 1)
\end{aligned}$$

Similarly, to find the limiting distribution of $X^{(N)}$ under the martingale measure induced by using the asset S as a numeraire:

$$\mathbb{E}^{\mathbb{Q}}[\frac{B_{t,k}}{S_{t,k}} | \mathcal{F}_{k-1}] = \frac{B_{t,k-1}}{S_{t,k-1}}$$

Set $q_s = \mathbb{Q}^S(\epsilon_k = 1)$

$$\begin{aligned}
\frac{B_{t,k}}{S_{t,k}} &= q_s \frac{B_{t+1,k}}{S_{t+1,k}} + (1 - q_s) \frac{B_{t+1,k+1}}{S_{t+1,k+1}} \\
\frac{B_{t,k}}{S_{t,k}} &= \frac{B_{t,k} e^{r\Delta t}}{S_{t,k} e^{r\Delta t + \sigma\sqrt{\Delta t}}} q_s + \frac{B_{t,k} e^{r\Delta t}}{S_{t,k} e^{r\Delta t - \sigma\sqrt{\Delta t}}} (1 - q_s) \\
q_s &= \frac{1 - e^{\sigma\sqrt{\Delta t}}}{e^{\sigma\sqrt{\Delta t}} - e^{-\sigma\sqrt{\Delta t}}} \\
q_s &= \frac{1}{2} + \frac{1}{4}\sigma\sqrt{\Delta t} + O(\Delta t) \quad \text{by applying Taylor expansion}
\end{aligned}$$

Then,

$$\begin{aligned}
\mathbb{E}^{\mathbb{Q}^s}[e^{u_k}] &= e^{u\sigma\sqrt{\Delta t}}\left(\frac{1}{2} + \frac{1}{4}\sigma\sqrt{\Delta t}\right) + e^{-u\sigma\sqrt{\Delta t}}\left(\frac{1}{2} - \frac{1}{4}\sigma\sqrt{\Delta t}\right) + O(\Delta) \\
&= (1 + u\sigma\Delta t + \frac{1}{2}u^2\sigma^2\Delta t)\left(\frac{1}{2} + \frac{1}{4}\sigma\sqrt{\Delta t}\right) + (1 - u\sigma\Delta t + \frac{1}{2}u^2\sigma^2\Delta t)\left(\frac{1}{2} - \frac{1}{4}\sigma\sqrt{\Delta t}\right) + O(\Delta t) \\
&= 1 + \left(\frac{1}{2}u\sigma^2 + \frac{1}{2}u^2\sigma^2\right)\Delta t + O(\Delta t) \\
&= e^{(\frac{1}{2}u\sigma^2 + \frac{1}{2}u^2\sigma^2)\Delta t} + O(\Delta t) \\
\mathbb{E}^{\mathbb{Q}^s}[e^{uX^{(N)}}] &= e^{urT}\left(e^{(\frac{1}{2}u\sigma^2 + \frac{1}{2}u^2\sigma^2)\Delta t}\right)^N \\
&= e^{urT}\left(e^{(\frac{1}{2}u\sigma^2 + \frac{1}{2}u^2\sigma^2)T}\right) \\
&= e^{(u(r + \frac{1}{2}\sigma^2)T + \frac{1}{2}u^2\sigma^2T)} \\
X^{(N)} &\overset{\mathbb{Q}^s}{\sim} \mathcal{N}\left((r + \frac{1}{2}\sigma^2)T, \sigma\sqrt{T}\right) \\
X^{(N)} &\xrightarrow[N \rightarrow \infty]{d} (r + \frac{1}{2}\sigma^2)T + \sigma\sqrt{T}Z, \quad Z \overset{\mathbb{Q}^s}{\sim} \mathcal{N}(0, 1)
\end{aligned}$$

(3) Hedging Assumptions

To construct a hedging strategy for an American put option using asset S_t and the bank account, we need to determine the weight needed to be invested into the two assets.

$$\begin{array}{ccc}
& & (2) P_{t+\Delta t, k} = \alpha_{t, k} S_{t+\Delta t, k} + \beta_{t, k} e^{r\Delta t} \\
& \nearrow & \\
(1) P_{t, k} = \alpha_{t, k} S_{t, k} + \beta_{t, k} 1 & & \\
& \searrow & \\
& & (3) P_{t+\Delta t, k+1} = \alpha_{t, k} S_{t+\Delta t, k+1} + \beta_{t, k} e^{r\Delta t}
\end{array}$$

Rearrange (2) and (3) we get:

$$\begin{aligned}
(2) \quad & \alpha_{t, k} S_{t+\Delta t, k} + \beta_{t, k} e^{r\Delta t} - P_{t+\Delta t, k} = 0 \\
(3) \quad & \alpha_{t, k} S_{t+\Delta t, k+1} + \beta_{t, k} e^{r\Delta t} - P_{t+\Delta t, k+1} = 0
\end{aligned}$$

Equate the two equations and we get $\alpha_{t, k} = \frac{P_{t+\Delta t, k} - P_{t+\Delta t, k+1}}{S_{t+\Delta t, k} - S_{t+\Delta t, k+1}}$, for $t \in [0, T)$. When at expiry ($t = T$), the strategy is to either hold the stock or not. Thus, $\alpha_T = -\mathbb{1}(K - S_T \geq 0)$

We can calculate $\beta_{t, k}$ from (1) $\beta_{t, k} = \alpha_{t, k} S_{t, k} - P_{t, k}$

And finally, the value of the hedging portfolio is $V_{t, k} = \alpha_{t, k} S_{t, k} + \beta_{t, k} 1$

2.2 Exercise Boundary

In this section, we evaluate the exercise boundary of an American put option. The exercise boundary can be defined as the set of the underlying asset's prices at which it is optimal to exercise at each time step up to the maturity date.

Recall that for American put options, contract holders have the right to exercise early. Therefore, at each time step τ ($\forall \tau < T$), the payoff takes the maximum between the strike price K and the spot price S_τ .

$$f(S_\tau) = (K, S_\tau)_+$$

As a result, the value of an American put at τ is given by:

$$P_\tau = (\text{Holding Value}, \text{Intrinsic Value})_+$$

Where:

$$\text{Holding Value} = PV((\text{Expected Future Payoff}_{s_{t>\tau}}))$$

$$\text{Intrinsic Value} = (0, K - S_\tau)_+$$

Our exercise boundary is constructed in such a way that at each time point, we mark the maximum Spot price S_t^* at which the exercising condition is met, i.e. the intrinsic value exceeds the holding value.

We pass the following set of parameters into the model:

Table 1: Assumptions Table

Time to maturity	$T = 1$
Initial asset price	$S_0 = \$10$
Dividend yield	$\mu = 5\%$
Volatility	$\sigma = 20\%$
Risk-free rate	$r = 2\%$
Time steps	$N = 5000$
Strike price	$K = \$10$

We plot the exercise boundary as a function of t .

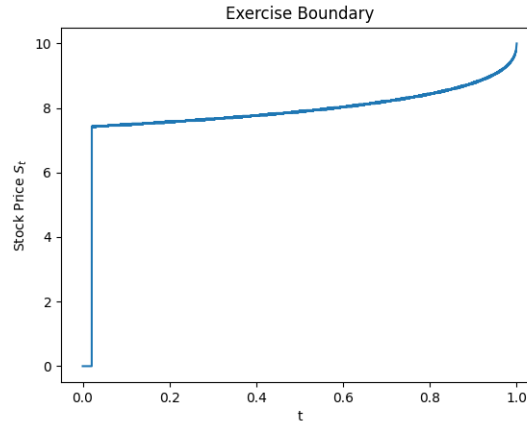


Figure 1: Exercise Boundary

The exercise boundary is a continuously increasing function of time t , which gradually converges to the strike price (K) as we approach the expiry date of the contract.

The rate of convergence of boundary price increases along with Time t , this is because as we approach the expiry date, the holding value of an American option increases as a result of shorter discounting period. The closer we get to the end point, the more boundary price gets pushed towards the strike price K . Intuitively, one would favour holding a position in an American put as opposed to exercising it, when time to expiry is longer as there's more room for potential gigantic price movements.

2.3 Hedging strategy

One strategy to hedge a long position in an American put option is replicating its payoff. Differing from a European option that can only be exercised at expiry, one must consider both the intrinsic and the potential holding value when hedging an American put.

Given access to asset S_t and the bank account in the market, our team will construct a portfolio of these two assets at each time points $t = 0, \frac{1}{4}, \frac{1}{2}, \frac{3}{4}, 1$ such that the portfolios' payoffs offset that of the put option.

As stated in the assumptions, the hedging portfolio has its value function given as: $V_{t,k} = \alpha_{t,k}S_{t,k} + \beta_{t,k}1$. To construct the hedging strategy, we need to first access the positions $\alpha_{t,k}$ invested in the stock and $\beta_{t,k}$ invested in the bank account.

To showcase how the weightings change with time, we calculated weightings at each time point, we then plotted the α, β positions as functions of Spot price S_t , this yields:

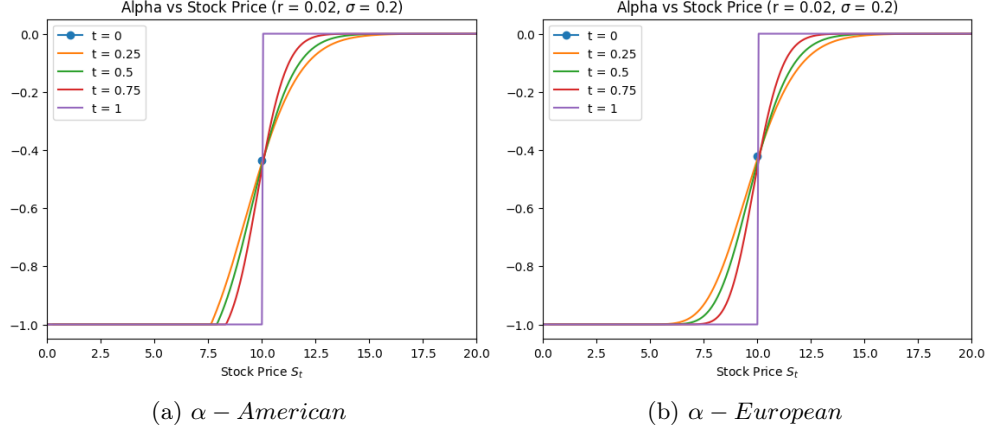


Figure 2: α Positions

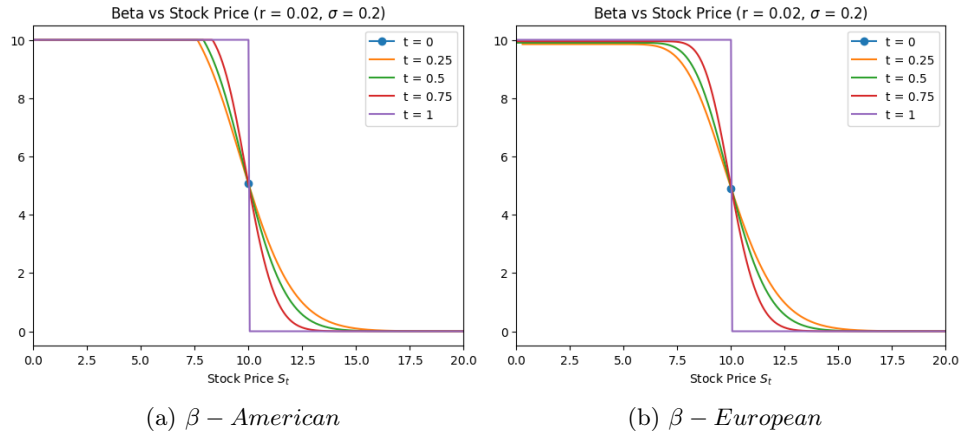


Figure 3: β Positions

A few observations based on **Figure 2 - 3**:

- α positions follow the same shape as the Delta of put options Δ_p , as the option moves from deep ITM to deep OTM, α moves from -1 towards 0;
- α and β positions display an inverse relationship, which holds as per the assumptions of a self-financing strategy;
- As time points approach 1, the slopes of both graphs become steeper;
- At the final time point $T = 1$, we would either hold or not hold the put contract based on the strike price K and the final spot price S_T , so we see a vertical line at $S_t = 10$;

- The distinguishing element between American and European put options can be seen from the sharper jump around the exercising boundary for American put. Intuitively, at each time point, contract holders for American put may choose to exercise pre-expiry if the exercising condition is met.

We then construct the portfolio tilted with the weighting parameters. To evaluate the payoff of our portfolio with respect to the Spot price S_t , we plotted it as a function of S_t at each time point:

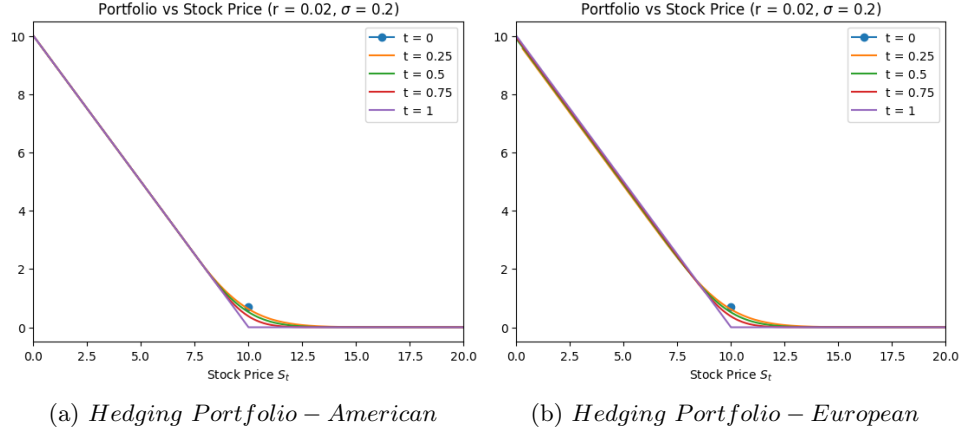


Figure 4: *Hedging Positions*

Overall, both portfolios follow the same pattern, demonstrating a negative correlation to spot price S_t .

2.4 Simulation

After having a concrete outlook of the exercising conditions and boundaries, we are interested in learning the potential profit and loss in addition to the chances of early exercising for American put holders. Before running the estimation, we first need to simulate sample paths for the Spot price S_t .

We first drew the same set of parameters from **Table 1**. We ran 10,000 stochastic simulations of the sample paths, which follow the stock price process and distribution outlined in **Assumption. (1) Stock Distribution**. To get a graphical intuition of the asset price distribution, we plotted the sample paths along with the exercise boundary.

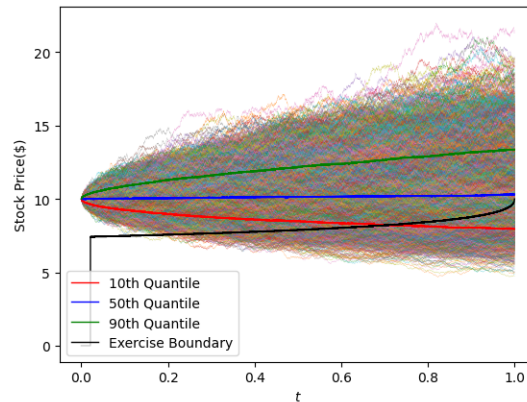


Figure 5: *Simulation Results*

Here, we see that in over half of the scenarios, one will not early exercise the American put option. However, as we approach expiry, the likelihood of crossing under the exercise boundary into the stop region would increase. As the profit and loss of the American put are properly defined by the difference between

its discounted payoff and the price of the put option, we pose a hypothesis that under current market conditions, we are more likely to incur a loss holding this put option.

For the purpose of evaluation, aside from the ordinary simulation, we also conducted a parameter adjustment for the simulation. The analysis set-up and results will be discussed in **Section 3.2 Parameter Adjustments for KDE**.

2.5 Estimation

Lastly, we attempt to perform estimations on the long American put position stated above. To give a concise view of the dynamics, we modelled the distribution of profit and loss along with the exercise time using the Kernel Density Estimation method. We included all the simulated results for the KDE of profit and loss. On the other hand, we excluded all the paths that are not exercised by the maturity for the KDE of exercise time.

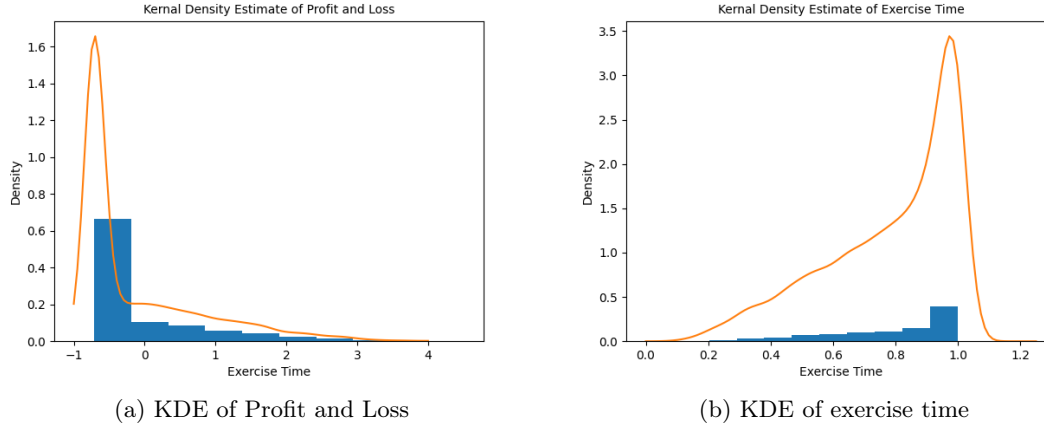


Figure 6: Kernel Density Estimates

Based on our estimates, the expected loss on the put option is around $-\$0.1344$, and the expected exercise time is around 0.7860. The profit and loss distribution is largely right-skewed, while exercise time is left-skewed. This is consistent with our hypothesis and observation that over half of the paths the option never gets exercised, thus resulting in a loss of premium amount.

3 Model Interpretation and Results

3.1 Scenario Analysis

To study how the model results vary as volatility and interest rate change, we implemented a sensitivity analysis. We came up with three sets of scenarios for each parameter, detailed as follows:

Table 2: Parameter Values

Risk-free rate r	Volatility σ
0.02	0.1
0.04	0.2
0.10	0.3

To start with, we analyze the exercising boundaries under each scenario:

As can be seen from **Figure 7**, the Exercise boundary exhibits a positive correlation with interest rate r and a negative correlation with volatility σ . We also see larger dispersion when adjusting the value of volatility σ . Our exercise boundary is more sensitive to changes in volatility.

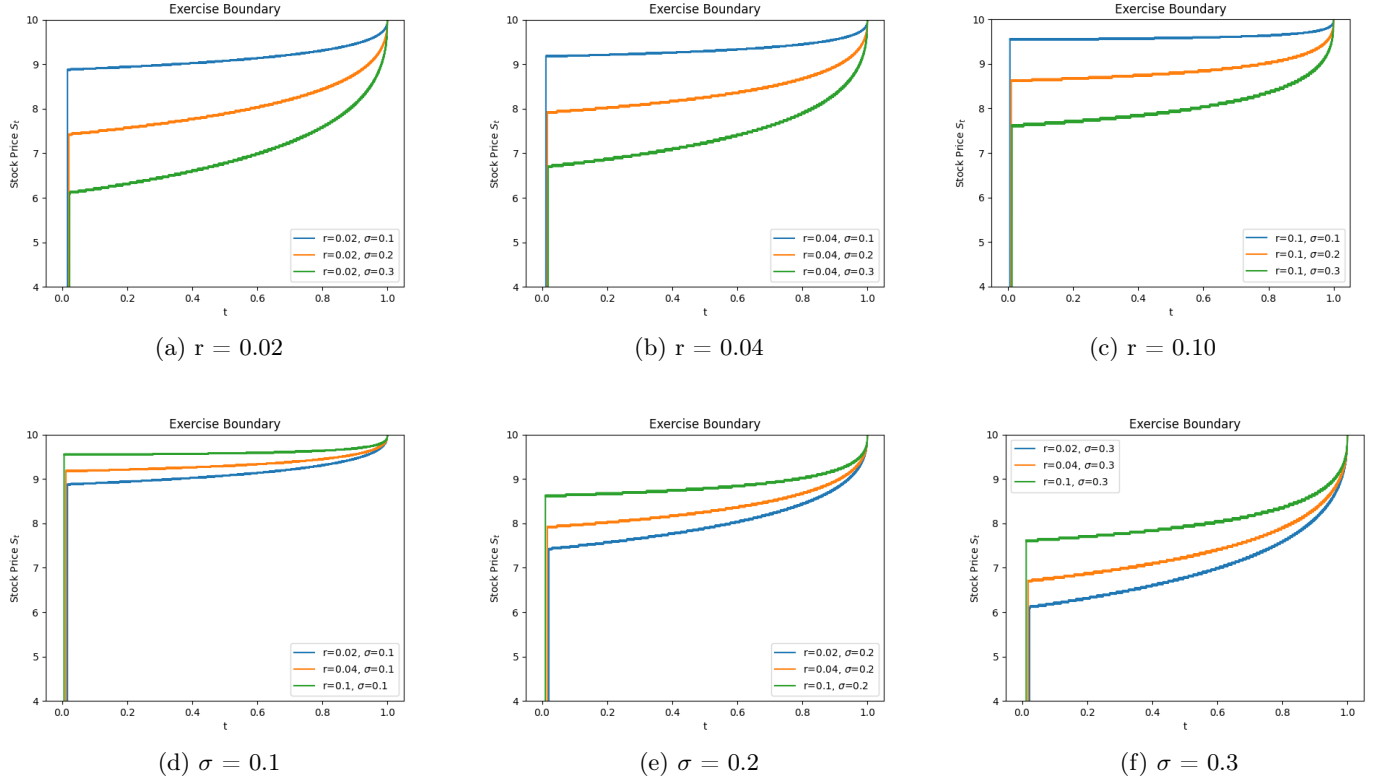


Figure 7: Exercise boundaries

Then we look into how the hedging positions behave under scenarios specified above.

(1). α plots:

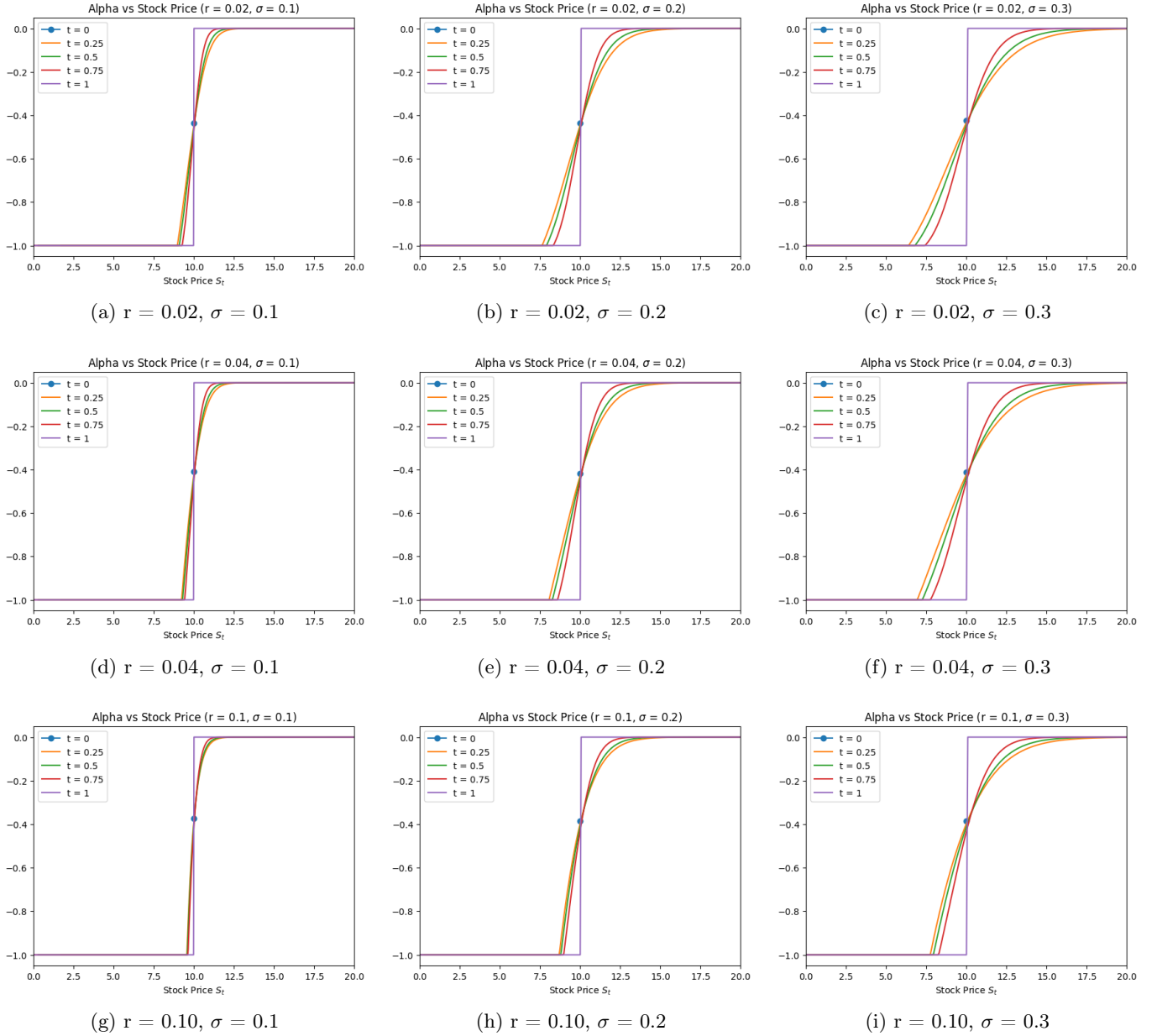


Figure 8: α positions

Here we draw similar conclusions to that of the exercise boundaries. The steepness of the slopes of α graphs is positively correlated to interest rate r and negatively correlated to volatility σ . Additionally, α positions are more sensitive to changes in volatility than changes in interest rate.

(2). β plots:

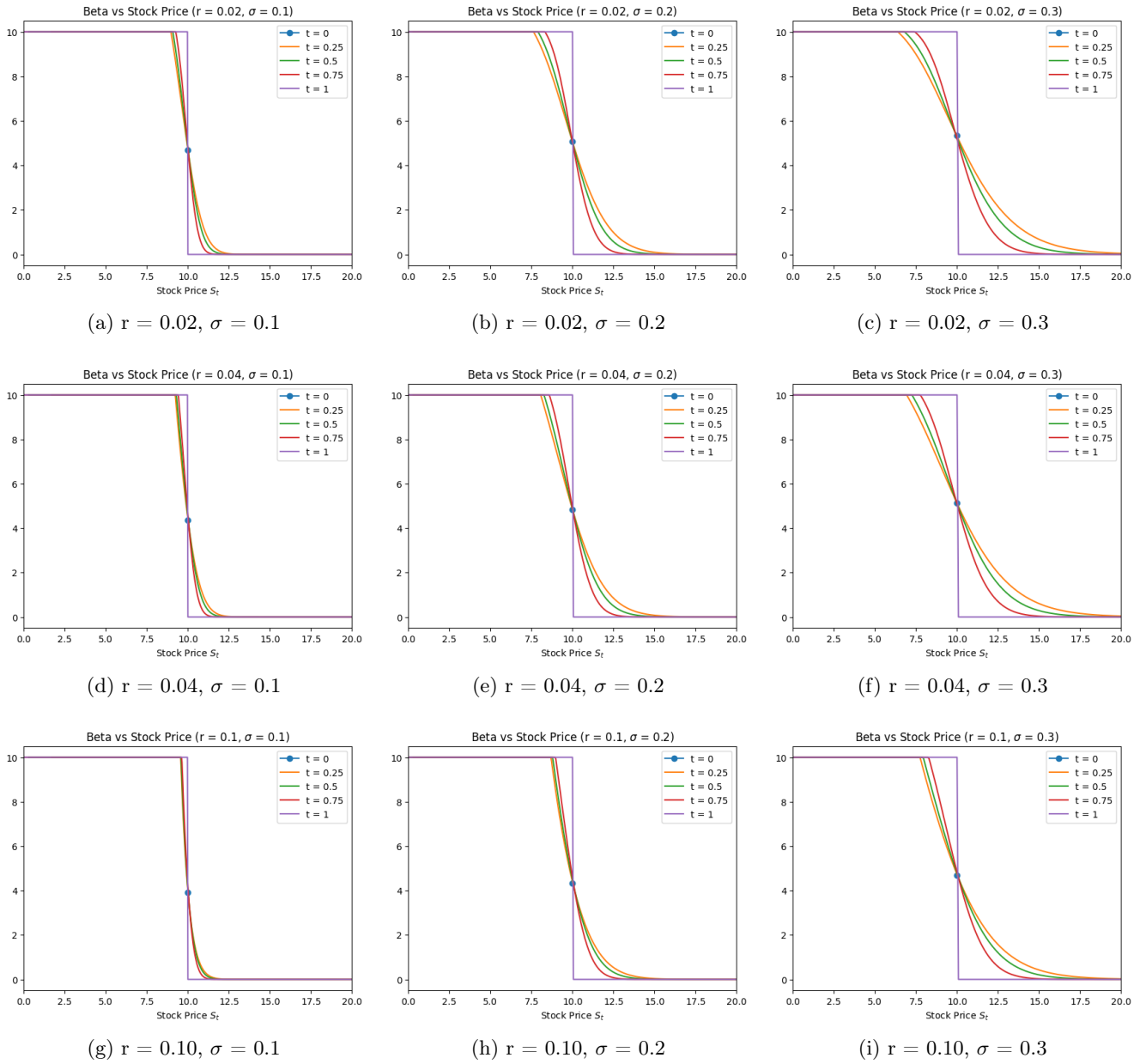


Figure 9: β positions

Not surprisingly, the graph flattens as volatility drops and steepens as interest rate surges. The β positions in our portfolio are also more sensitive to changes in volatility.

Now that we have shown results for both α and β , let's re-construct hedging portfolios based on all sets of parameters:

(3). Portfolio plots:

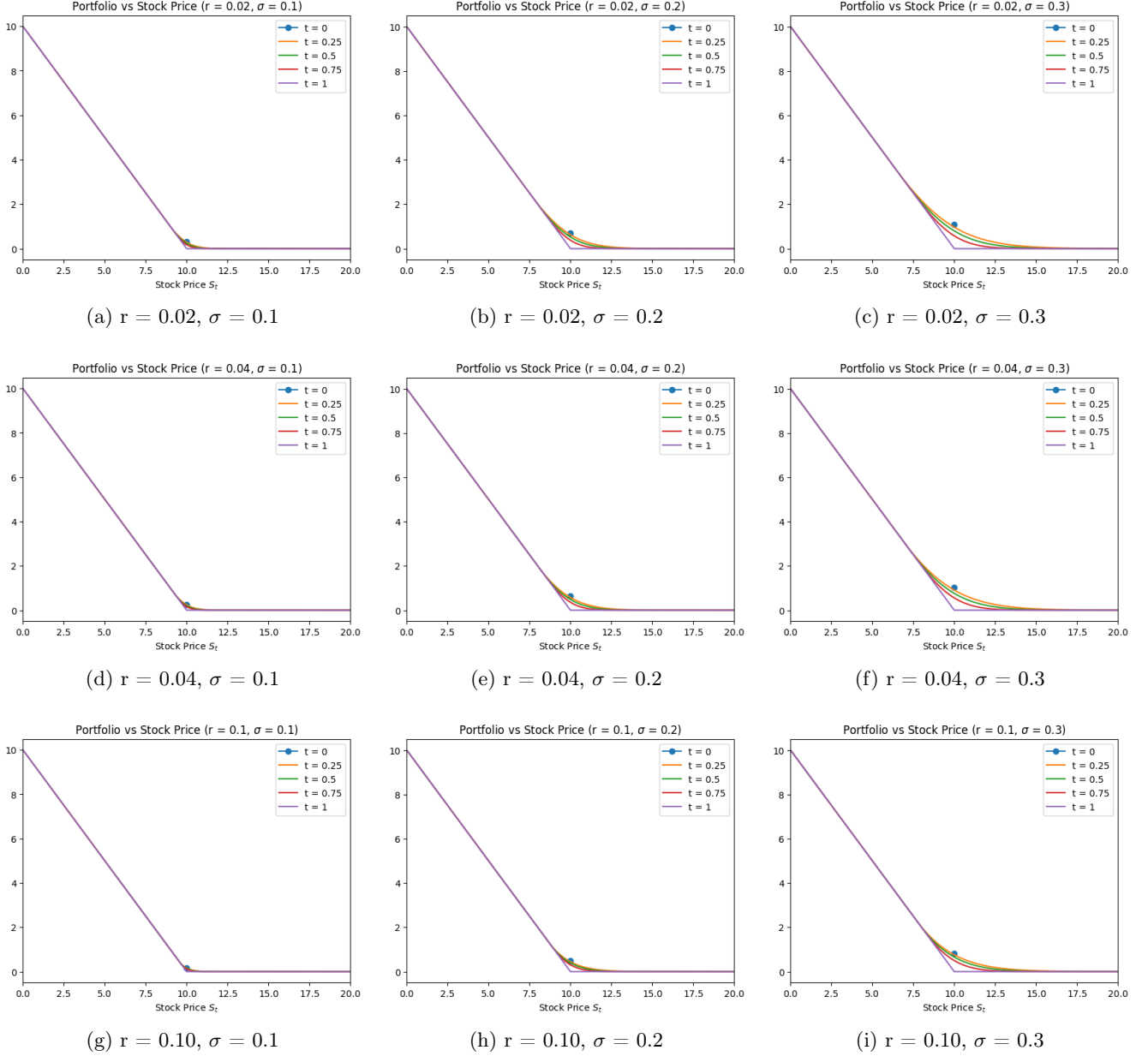


Figure 10: Portfolio positions

Overall, when the interest rate falls or when volatility rises, we see that the portfolio value function deviates further away from the terminal value function (when $T = 1$).

After illustrating the evolution of exercise boundaries and hedging positions under various scenarios, it is worthwhile to understand the intuition behind such distinctions.

3.2 Parameter Adjustments for KDE

To study how the estimations vary across different sets of model parameters, we formulate the distributions using different sets of parameter assumptions. For each case, we investigated the effect of changing one parameter while holding the other parameters constant as in the base model setting. Within each case, we also outline the parameter effects; the list of parameters adjusted is as follows: divided yield μ , interest

rate r , Strike price K and volatility σ . The detailed parameter assumptions are as follows:

Table 3: KDEs under different volatility

Strike price	Dividend yield μ	Interest rate r	Volatility σ
\$8	0.01	0.005	0.1
\$9	0.03	0.01	0.15
\$10	0.05	0.02	0.2
\$11	0.07	0.03	0.25
\$12	0.09	0.035	0.3

Based on above parameter assumptions, we showcase the distributions as follow:

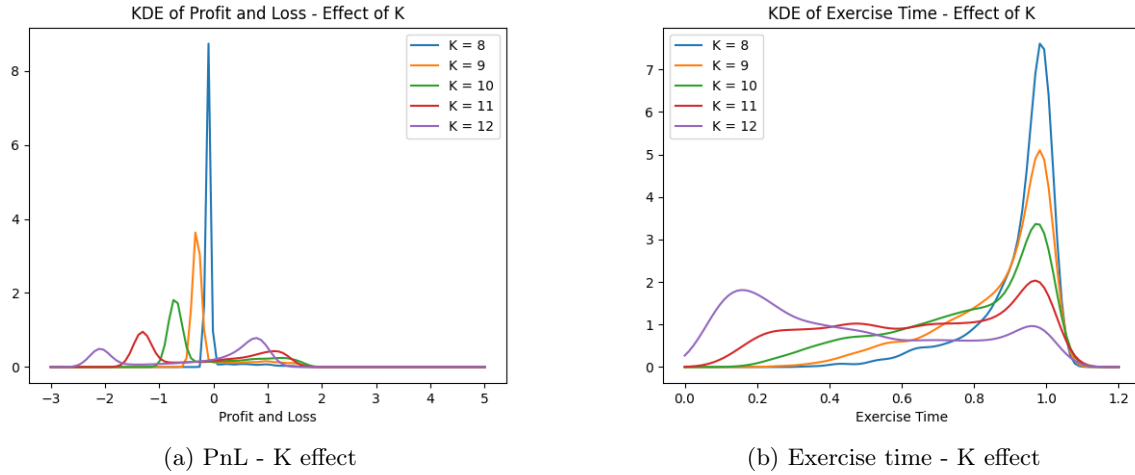


Figure 11: Effect of Strike price on KDEs

Looking at the profit and loss under each strike price K , we generally observe two peaks for each distribution. This is consistent across all scenarios. As K increases, the x coordinates of the first peaks representing the loss when contracts expire worthless gradually deteriorate, trending away from zero. Since we know that with a larger strike price comes a higher valuation in both the intrinsic and holding value, the loss amount described by the option premium (or price of the option) surges. Also, notice that at a lower strike price, the density of the first peak gets more significant since the put option is more likely to expire unexercised at lower strikes. Following the first peak, the second maximum point arrives at the positive side of the axis. This represents the gain when exercised prior to expiry. Inheriting from the rationale above, when we push the strike price up, chances of early exercising grow, which is reflected in the height of the peak (i.e. the density). However, valuation grows along, leading to a lower expected gain (i.e. lower x coordinate).

When accessing the strike price effect on exercise time, we see a robust jump around time $T = 1$ for all K s as a large portion of paths never gets exercised. Distributions are generally left-skewed, which is also consistent across all scenarios. An interesting observation is found at earlier time steps. Note that prior to the mid-point ($T = 0.5$), the density of exercise time fluctuates. The higher the strike, the more significant the density gets. As explained above, the likelihood of exercising improves with the strike price. At $K = 12$, which is the largest strike we tested, options are more likely to be exercised early than expired worthless. This coincides with the shape of the PnL distribution as well.

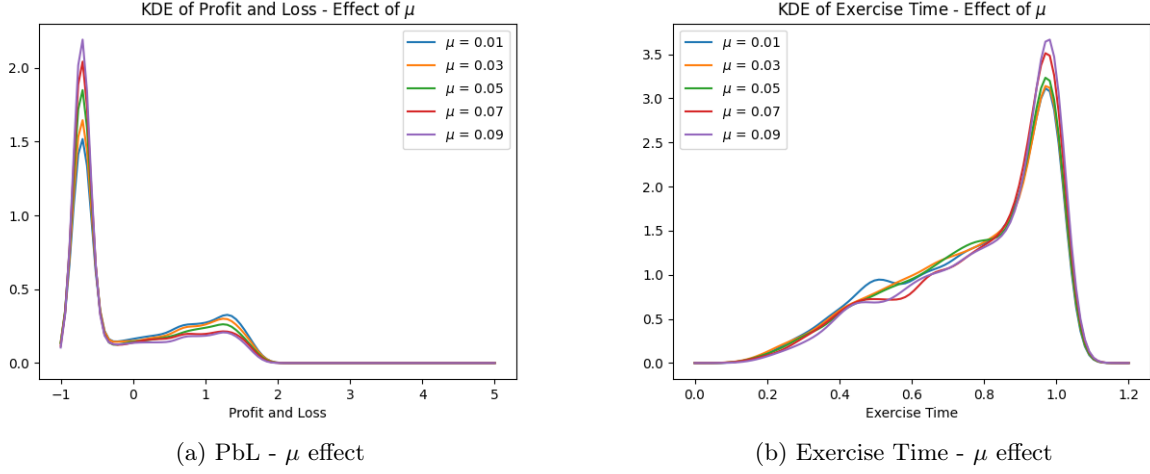


Figure 12: Effect of dividend yield on KDEs

Next, we investigate the effect of dividend yield μ on the profit and loss. Unlike the strike price effect, the most (density-wise) significant loss and gain are agreed across all values of μ (i.e. the x-coordinates of the peaks are stable). Recall that $P(\epsilon_k = \pm 1) = \frac{1}{2} \pm (1 + \frac{(\mu-r) - \frac{1}{2}\sigma^2}{\sigma})$, changes in μ are reflected in the probability measure for $P(\epsilon_k = \pm 1)$, more specifically the underlying has higher upside potential when passed with a large μ . For a put option, one has less chance of early exercising if the dividend yield gets higher, which is reflected by the higher density at a loss and consequentially lower density at a gain. The above logic can be applied to explain the effect on exercise time. More options expire without exercising at larger dividend yield μ .

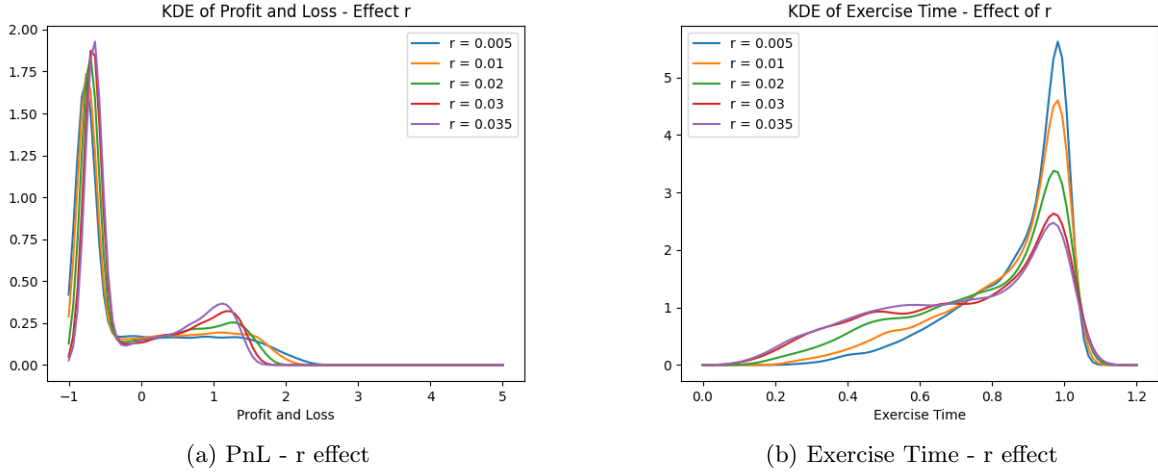


Figure 13: Effect of interest rate on KDEs

The effect of interest rate is, in fact, inversely related to that of the dividend. From the P probability measure stated above, we immediately see that interest rate restricts the up movement of the underlying. Note that this is, however, only related to the probability measure of up move in stock price and nothing about the discounting, as the $e^{r\Delta t}$ term in the asset price process cancels out the discounting factor.

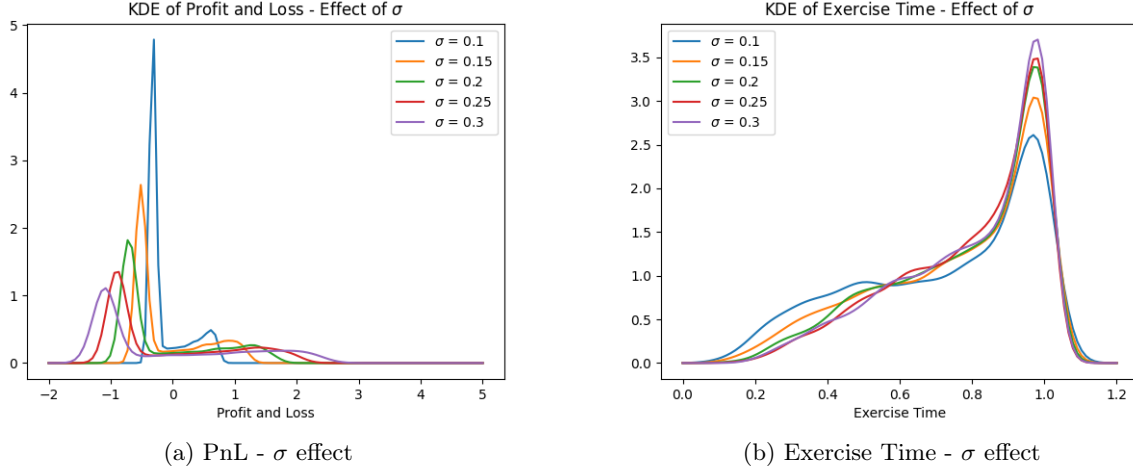


Figure 14: Effect of volatility on KDEs

Lastly, we attempt to describe the volatility effect. Adjusting volatility in the simulation model, we found that the profit and loss peaks also shift. However, the underlying rationale is rather different: As Figure 7, lower σ widens the continuation region for the exercise boundary, leading to less chance of early exercising and larger potential loss (reflected in the region under the loss peak). Hence the intuition aligns with our observation. Volatility yields a negative effect on profit and loss and a positive impact on exercise time.

3.3 Scenario Analysis for KDE

In a similar fashion, we attempt to conduct scenario analysis on the Kernel Density Estimation where value of realized volatility changes. To set up the analysis, we adjust the value of realized volatility to mimic different market conditions, horizontally applying the same parameter assumptions in **Table 1** and perform estimations under each scenario. Assuming we have longed the option with a volatility of $\sigma = 20\%$, and for the purpose of consistency we would also adapt the $\sigma = 20\%$ exercise boundary in our trading strategy. The set of realized volatility to test on are $\sigma = 10\%, 15\%, 20\%, 25\%, 30\%$. Iterating the estimation at each value of σ yields:

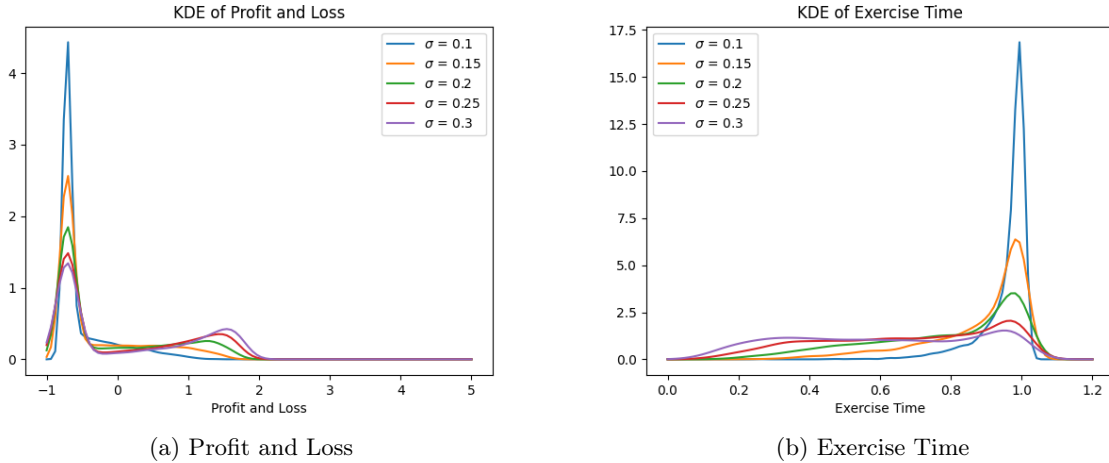


Figure 15: Scenario test on KEDs

From **Figure 15**, we observe the volatility effect on our estimations. As realized volatility increases, expected profit and loss follow, exhibiting a positive correlation. While the estimated exercise time shortens with rising volatility.

Table 4: KDEs under different volatility

	Estimated profit and loss	Estimated exercise time
$\sigma = 0.10$	\$(0.5059)	0.9568
$\sigma = 0.15$	\$(0.3095)	0.8762
$\sigma = 0.20$	\$(0.1319)	0.7878
$\sigma = 0.25$	\$0.0348	0.6884
$\sigma = 0.30$	\$0.1578	0.5985

Under different realized volatility, the dispersion in profit and loss and exercise time widens. A more volatile market condition gives rise to the estimated profit and loss in our model. Additionally, predicted exercise time shortens as investors tend to exercise their options more frequently.

4 Conclusion

Throughout the paper, we attempt to build a comprehensive outlook on the dynamics of a typical American put option. We started with the assumption settings on the stock price distribution and risk-neutral probability and then investigated the exercising condition and hedging strategy for American put along with their sensitivity to parameter adjustments. Based on our results, both the exercise boundary and hedging strategy are more sensitive to volatility changes than interest rate changes. This implies that the uncertainty in pricing and hedging arise more from the dynamics of the underlying itself than from the condition of the market. In a nutshell, contingent claims written on more volatile underlying assets tend to have lower exercise boundaries, or put differently, a narrower stopping region paired with a wider continuation region.

To consolidate our discovery and forge a better understanding of profit and loss, we ran stochastic simulations in addition to Kernel Density Estimations on the behaviour of profit and loss and exercise time for the American put. Under a base set of parameters, our model predicts a loss on the option contract, with a strong likelihood of never exercising or exercising near expiry. Interpreting the model results when passed with various parameters, we conclude that among several factors, strike price and volatility of underlying yield have the greatest impacts on our estimations. While factors such as dividend yield μ and interest rate r don't really influence the profit and loss in terms of their amount, changing strike price K and volatility σ would cast material impacts on the expected profit and loss. It follows that a higher strike price increases the spread between the profit and loss on the distribution and, consequentially, earlier exercise time. Alternatively, volatility hikes deteriorate expected profit and losses and extend exercise time.